

DOCTORAL THESIS

Use of intra-procedural fusion imaging combining contrast-enhanced ultrasound using a perflubutane-based contrast agent and auto sweep three-dimensional ultrasound for guiding radiofrequency ablation and evaluating its efficacy in patients with hepatocellular carcinoma

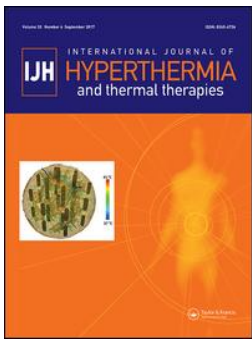
(肝細胞癌に対するラジオ波焼灼療法のガイダンスと治療効果判定における auto sweep による三次元超音波とペルフルブタン造影超音波の融合画像の術中使用の検討)

September, 2020
(2020 年 9 月)

Katsuyuki Sanga
三箇 克幸

Gastroenterology
Yokohama City University Graduate School of Medicine
横浜市立大学 大学院医学研究科 医科学専攻 消化器内科学

(Doctoral Supervisor : Shin Maeda, Professor)
(指導教員 : 前田慎教授)



Use of intra-procedural fusion imaging combining contrast-enhanced ultrasound using a perflubutane-based contrast agent and auto sweep three-dimensional ultrasound for guiding radiofrequency ablation and evaluating its efficacy in patients with hepatocellular carcinoma

Katsuyuki Sanga, Kazushi Numata, Hiromi Nihonmatsu, Katsuaki Ogushi, Hiroyuki Fukuda, Makoto Chuma, Hiroshi Hashimoto, Norihiro Koizumi & Shin Maeda

To cite this article: Katsuyuki Sanga, Kazushi Numata, Hiromi Nihonmatsu, Katsuaki Ogushi, Hiroyuki Fukuda, Makoto Chuma, Hiroshi Hashimoto, Norihiro Koizumi & Shin Maeda (2020) Use of intra-procedural fusion imaging combining contrast-enhanced ultrasound using a perflubutane-based contrast agent and auto sweep three-dimensional ultrasound for guiding radiofrequency ablation and evaluating its efficacy in patients with hepatocellular carcinoma, *International Journal of Hyperthermia*, 37:1, 202-211, DOI: [10.1080/02656736.2020.1729422](https://doi.org/10.1080/02656736.2020.1729422)

To link to this article: <https://doi.org/10.1080/02656736.2020.1729422>



© 2020 The Author(s). Published with license by Taylor & Francis Group, LLC



Published online: 18 Feb 2020.



Submit your article to this journal [↗](#)



Article views: 331



View related articles [↗](#)



View Crossmark data [↗](#)

Use of intra-procedural fusion imaging combining contrast-enhanced ultrasound using a perflubutane-based contrast agent and auto sweep three-dimensional ultrasound for guiding radiofrequency ablation and evaluating its efficacy in patients with hepatocellular carcinoma

Katsuyuki Sanga^{a,b}, Kazushi Numata^a, Hiromi Nihonmatsu^a, Katsuaki Ogushi^a, Hiroyuki Fukuda^a, Makoto Chuma^a, Hiroshi Hashimoto^c, Norihiro Koizumi^d and Shin Maeda^b

^aGastroenterological Center, Yokohama City University Medical Center, Yokohama, Japan; ^bDepartment of Gastroenterology, Graduate School of Medicine, Yokohama City University, Yokohama, Japan; ^cUltrasound Systems Engineering, GE Healthcare Japan Corporation, Hino-shi, Japan; ^dDepartment of Mechanical and Intelligent Systems Engineering, Graduate School of Informatics and Engineering, School of Informatics and Engineering, The University of Electro-Communications, Choufu-shi, Japan

ABSTRACT

Purpose: This study evaluated the usefulness of intraprocedural contrast-enhanced ultrasound (CEUS)/ultrasound (US) fusion imaging using a perflubutane-based contrast agent combined with preprocedural auto sweep three-dimensional US to obtain volume data for guidance and evaluation of the therapeutic efficacy of radiofrequency ablation (RFA).

Methods: This uncontrolled clinical trial included 50 hepatocellular carcinomas (HCCs) with a mean diameter of 15.3 mm that had been treated by RFA. The efficacy of RFA was evaluated by CEUS/US fusion imaging during the procedure. If the ablation was deemed to be inadequate, further ablation was performed until adequate ablation was achieved. Contrast-enhanced computed tomography (CECT) or contrast-enhanced magnetic resonance imaging (CEMRI) was performed a month after RFA, and the images obtained using each modality were reviewed to evaluate the efficacy of RFA.

Results: Thirty-three of the 50 lesions were evaluated by CEUS/US fusion imaging as having been adequately ablated after the first RFA procedure. The ablation was evaluated as inadequate in the remaining 17 lesions, for which additional ablation was performed. Ninety-eight (49/50) of all HCCs were evaluated as having been eventually adequately ablated on intraprocedural CEUS/US fusion imaging. The concordance rate for evaluations between intraprocedural CEUS/US fusion imaging and CECT/CEMRI performed 1 month after RFA was 88% (44/50). The kappa value for agreement between the two methods of evaluation was 0.792.

Conclusion: Intraprocedural fusion imaging combining CEUS and auto sweep three-dimensional US appears to be a useful modality for RFA guidance and evaluation of therapeutic efficacy of RFA in patients with HCC.

ARTICLE HISTORY

Received 16 October 2019
Revised 1 February 2020
Accepted 5 February 2020

KEYWORDS

Fusion imaging; contrast-enhanced ultrasound; perflubutane-based contrast agent; hepatocellular carcinoma; radiofrequency ablation

Introduction

Contrast-enhanced computed tomography (CECT) and contrast-enhanced magnetic resonance imaging (CEMRI) are the most widely used imaging techniques for evaluation of the therapeutic efficacy of radiofrequency ablation (RFA) for hepatocellular carcinoma (HCC) [1–4]. However, neither of these imaging techniques can be performed during the RFA procedure to evaluate its therapeutic efficacy. The recent European Federation of Societies for Ultrasound in Medicine and Biology guidelines have highlighted the role of contrast-enhanced ultrasound (CEUS) as a cost-effective technique with a good safety profile, not only for characterization and detection of focal liver lesions, but also for monitoring tumor response after curative, locoregional or systemic treatment for HCC [5–7]. However, the ablation margin can be hard to

determine by CEUS because of the difficulty in identifying the edge between the ablated HCC and the ablated adjacent liver parenchyma using this imaging modality alone [8,9].

In contrast, disappearance of the vascularity of HCC after RFA can be evaluated by fusion imaging using a combination of CEUS and CECT [10]/CEMRI [11] because CEUS and arterial-phase CECT or hepatobiliary-phase CEMRI, used as reference, allows the location of the treated HCC to be visualized [10,11]. In our studies, we have used global positioning system (GPS) marks, whereby small green cross graphics appear simultaneously in CECT (arterial phase) [10]/CEMRI (hepatobiliary phase) [11] and CEUS, enabling the location of the ablated HCC to be confirmed and differentiated from the adjacent ablated liver parenchyma. Fusion imaging combining CEUS and arterial-phase CECT as

reference appears to be a useful method for evaluating the therapeutic efficacy of RFA for hypervascular HCCs detected using conventional US [10]. Fusion imaging combining CEUS and hepatobiliary-phase CEMRI also appears to be useful for evaluating the therapeutic efficacy of RFA for HCCs identified as having isoechoic or unclear margins by conventional US [12]. The usefulness of fusion imaging combining CEUS and CECT/CEMRI for evaluating the therapeutic efficacy of RFA has been reported by several investigators [13,14]. The reported concordance rate for the results of the RFA efficacy evaluation between intraprocedural CEUS and CECT/CEMRI fusion imaging and CECT/CEMRI performed within 30 days after RFA was 91.1% (72/79) [13].

However, because of registration error, a fusion image does not always precisely correspond to the US image. One of the reasons for registration error is the difference in timing of breath-holding during image acquisition by each modality. CT images are usually obtained at the end of inspiration with a breath-hold whereas magnetic resonance images are obtained at the end of expiration after a breath-hold. US images are acquired with patients holding their breath during gentle respiration, which is adequate for puncture of the lesion for RFA. Therefore, the image registration error associated with use of CEUS/CECT or CEMRI fusion imaging can be reduced by CEUS/US fusion imaging, namely, real-time CEUS combined with pretreatment three-dimensional US to obtain volume data, because the breath-hold time is almost the same. The usefulness of CEUS/US fusion imaging for evaluation of the therapeutic efficacy of RFA has been reported previously [15]; however, the US volume data in that study were obtained by manual sweep three-dimensional US. For a sonographer who is not familiar with that modality, it may be difficult to maintain a constant speed of scanning without the transducer slipping upon hitting a rib in manual-sweep three-dimensional US, which may result in deformed volume data and, consequently, inaccurate evaluation of the therapeutic efficacy of RFA. In contrast, accurate US volume data can be obtained with three-dimensional US in the auto sweep ([®]AutoSweep; GE Healthcare, Ltd. Chicago, IL) because the sonographer can scan the tumor and surrounding liver parenchyma at a constant scanning speed without needing to consider the presence of a rib, which allows more accurate evaluation of the therapeutic efficacy of RFA. However, as of now, there are no reports on evaluation of the therapeutic efficacy of RFA by CEUS/US fusion imaging (with the volume data obtained by AutoSweep three-dimensional US) for HCCs detected on conventional US.

In this study, we compared the usefulness of intraprocedural CEUS/US fusion imaging (using the US volume data obtained by AutoSweep three-dimensional US) for guiding RFA and evaluating its therapeutic efficacy with that of CECT or CEMRI performed 1 month after RFA.

Materials and methods

Subjects

This uncontrolled clinical trial was conducted with the approval of our institutional review board and in compliance

with the principles of the Declaration of Helsinki after obtaining informed consent from each of the participating patients. Between June 2017 and June 2018, we performed percutaneous RFA in 80 consecutive patients (with 93 HCCs) at our institution. Forty-three of these 80 patients (with 50 HCCs) were enrolled in the study.

The inclusion criteria were as follows: (1) age 20 years or older; (2) a maximum of three HCC lesions, each measuring less than 3 cm in diameter; (3) a platelet count of more than 5×10^4 /mL; (4) patient able to breath-hold; (5) a well-defined HCC margin on conventional US; (6) underlying hepatitis or cirrhosis classified as Child-Pugh grade A or B; (7) patient ineligible or unwilling to undergo surgery and (8) treatment scheduled with RFA alone.

The exclusion criteria were as follows: (1) HCC unable to be visualized adequately by CEUS because of bowel gas or the lesion being located more than 12 cm from the skin surface; (2) CECT or CEMRI unable to be performed because of a contraindication to use of intravenous iodinated contrast agents (allergic reaction or impaired renal function); (3) HCC located behind the portal vein, rendering accurate puncture of the lesion during RFA difficult; (4) presence of portal vein and/or hepatic vein tumor thrombi and (5) presence of extrahepatic metastases.

The remaining 37 patients (with 43 HCCs) were excluded for the following reasons: the lesion(s) showed isoechoic or unclear margins on conventional US and were treated by RFA under CEUS/CECT or CEMRI fusion imaging guidance (17 patients, 20 HCCs); conventional RFA was used to treat the lesions (20 patients, 23 HCCs); there was a contraindication to use of an intravenous iodinated contrast agent (seven patients, eight HCCs), the lesion(s) could not be evaluated in detail by CEUS (eight patients, nine HCCs); and difficulty breath-holding sufficiently during fusion imaging (five patients, six HCCs). Finally, 43 patients with 50 well-defined hyperechoic or hypoechoic HCC lesions on conventional US who underwent RFA under CEUS/US fusion imaging guidance were enrolled in the study.

Diagnosis of typical HCC

Diagnosis of typical HCC was established based on the radiological features of the lesion [16]. When a tumor did not show a typical enhancement pattern on CECT/CEMRI, the diagnosis was established by biopsy.

US imaging

Conventional US

First, we assessed the HCC lesions using the LOGIQ E9 ultrasound system (GE Healthcare, Ltd. Chicago, IL), with native tissue harmonic gray-scale imaging using a convex probe with a frequency of 1–6 MHz and a micro-convex probe with a frequency of 2–5 MHz (hereafter referred to as conventional US).

CEUS procedure

As previously reported [17,18], a perflubutane microbubble contrast agent (Sonazoid; Daiichi Sankyo, Tokyo, Japan) was

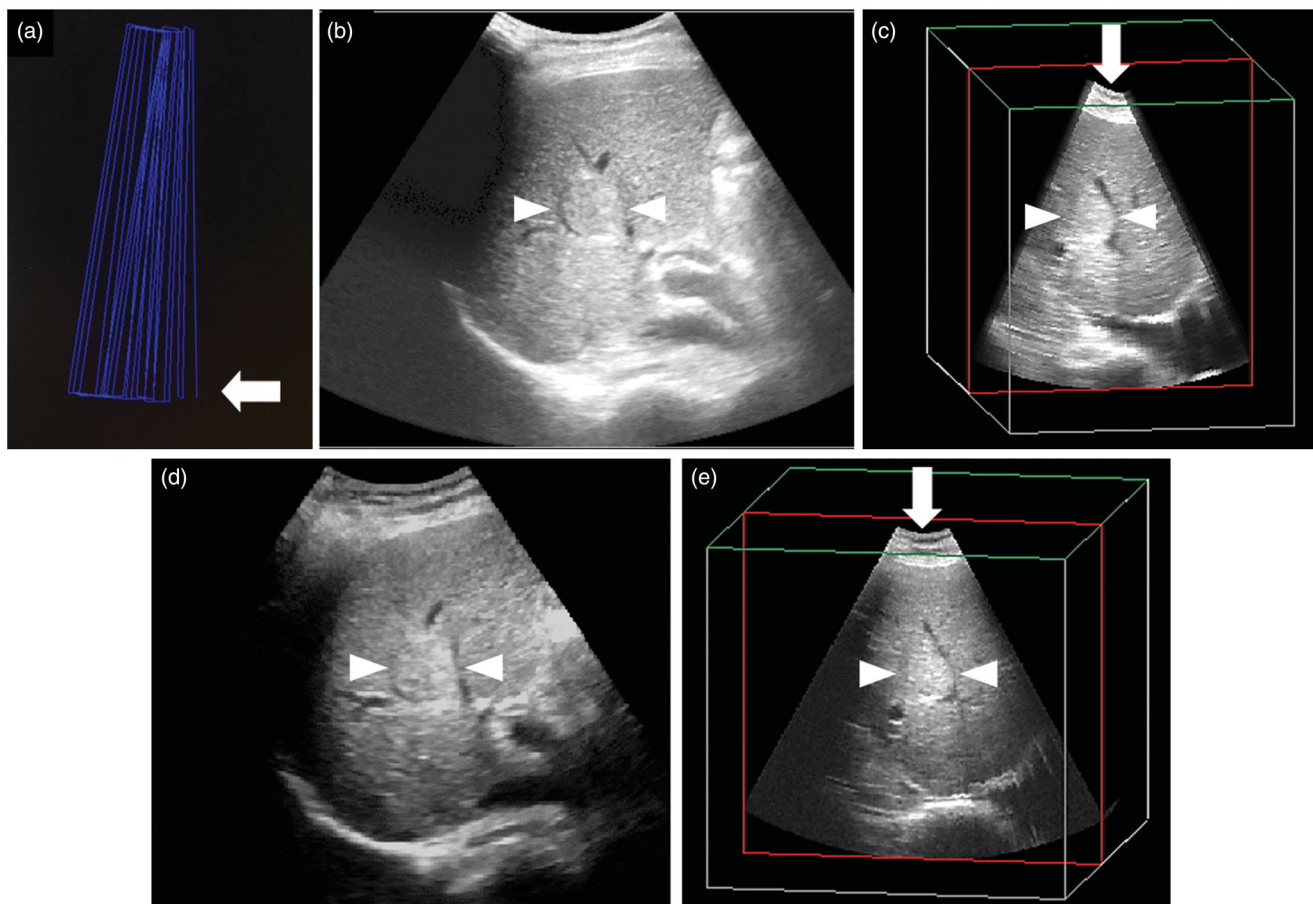


Figure 1. Comparison of three-dimensional ultrasound (3DUS) volume data images obtained by manual sweep scanning and AutoSweep scanning for an HCC lesion (maximum diameter, 28 mm) in segment VIII of the liver. (a) 3DUS volume data image obtained by manual sweep scanning. Blue lines indicate the locus of the manual sweep scanning. Arrow indicates the first frame of the manual sweep scanning. The distances between the blue lines are not equal, which indicates a non-constant scanning speed. (b) 3DUS volume data image obtained by manual sweep scanning. (c) 3DUS obtained by manual sweep allows viewing of the volume of interest in three orthogonal planes (this image shows plane B), which can be translated from right to left. The shape of the arc is not symmetrical due to the non-constant scanning speed (arrow). (d) US volume data image obtained by AutoSweep scanning. Comparison with the image in Figure 1(b) obtained by manual sweep shows that the images look almost the same. (e) 3DUS image obtained by AutoSweep allows viewing of the volume of interest in three orthogonal planes (this image shows plane B), which can be translated from right to left. Comparison with the image shown in Figure 1(c) obtained by manual sweep shows that the shape of the arc is symmetrical and the scanning range is slightly wider than that in the image shown in Figure 1(c) (arrow). Arrowhead indicates the margin of the HCC.

injected into an antecubital vein at a dose of 0.2 ml *via* a 24-gauge cannula and followed by injection of 2 ml of 5% glucose. CEUS images were acquired during three contrast phases, including the arterial phase (10–50 s after the start of injection), portal phase (80–120 s after the start of injection) and post-vascular phase (10 min after the start of injection). Using CEUS based on native tissue harmonic imaging at a low mechanical index (0.28) and a high frame rate (28–30 frames per second), the tumor vessels and staining could be evaluated in detail and in real time [17,18].

Fusion imaging

The fusion imaging system used in the study consisted of a position sensing unit mounted on an US unit, a magnetic transmitter, and a position sensor internally equipped with a US probe. The transmitter was placed on a stand so that the area being scanned was within the range of the transmitter. Using the position sensor attached to the transducer, the fusion feature allowed us to import pre-obtained volumetric Digital Imaging and Communication in Medicine (DICOM)

data and to register the US images with the pre-obtained volumetric digital images.

In this study, we used a convex volume probe with a frequency of 2–5 MHz to import pre-obtained three-dimensional US volume data obtained by AutoSweep and then fused the conventional US image and three-dimensional US volume data (Figures 1 and 2(a)). Scanning to obtain the three-dimensional US volume data was performed immediately prior to RFA under breath-holding with the patient kept immobilized.

To achieve adequate registration by minimizing the registration error while fusing conventional US or CEUS and the three-dimensional US images, we implemented the following modifications: (1) immobilization of the patient during the RFA procedure; (2) minimization of the distance between the magnetic transmitter and the position sensor and (3) fusion of the conventional US or CEUS and three-dimensional US images of the bifurcation of the portal vein obtained during a single breath-hold. After suitable registration of the conventional US or CEUS and three-dimensional US volume data, the results of conventional US or CEUS scanning were

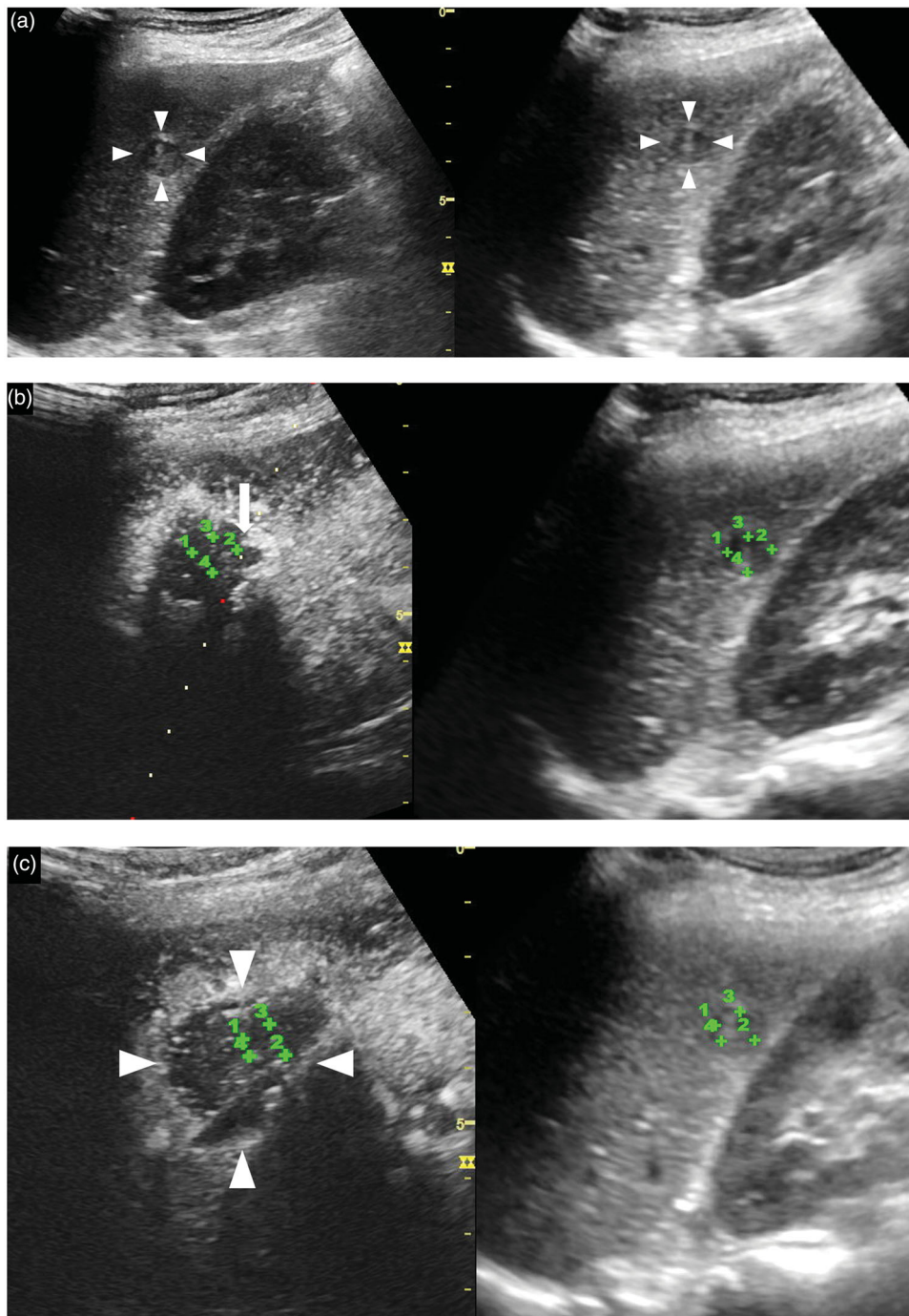


Figure 2. A 70-year-old woman with an HCC lesion (maximum lesion diameter, 13 mm) in segment VI of the liver. (a) Transcatheter fusion imaging, combining real-time conventional US imaging (left side) and AutoSweep three-dimensional ultrasound (3DUS) imaging to obtain volume data (right side), was performed prior to the RFA and the image(s) is presented on a single screen. The fusion image shows a hypoechoic lesion (arrowhead) in segment VI of the liver. (b) Transcatheter fusion imaging, combining arterial-phase CEUS imaging (left side) and AutoSweep 3DUS to obtain volume data (right side), was performed immediately after the RFA procedure, and the image(s) is presented on a single screen; the lesion was evaluated by fusion imaging with GPS marks. The green cross numbers 1–4 indicate the margin of the ablation area. The ablation margin was evaluated as inadequate because of the insufficient ablation margin (arrow), and additional ablation was performed under CEUS/US fusion imaging. (c) Immediately after the additional ablation, transcatheter fusion imaging, combining arterial-phase CEUS imaging (left side) and Auto Sweep 3DUS to acquire volume data (right side), was performed and the image(s) is presented on a single screen; this lesion was evaluated using fusion imaging with GPS marks. The green cross numbers 1–4 indicate the margin of the ablated HCC area. The ablation was evaluated as adequate, because no enhanced areas were visible within the entire tumor during the arterial phase and an ablative margin (arrowheads) was present around the entire tumor area during the arterial phase. Hepatobiliary phase EOB-MRI image obtained (d) before and (e) 1 month after the RFA. This lesion was judged as having been adequately ablated, because a low-signal area (arrowheads) was observed during the hepatobiliary phase in the low-signal area covering the area (arrow) seen in (d). Local tumor progression has not been identified during the 16 months that have elapsed since the RFA.

viewed at the same time as the three-dimensional US volume data. Furthermore, we used GPS marks (Figure 2(b,c)) to confirm the location of the HCC [17–22] and to identify the margin of the treated HCC for evaluation of the efficacy of

RFA immediately after the procedure. After registration of the CEUS and three-dimensional US images obtained during a single breath-hold, we set the GPS marks at the largest cut surface of the treated lesion, which was visualized as an HCC

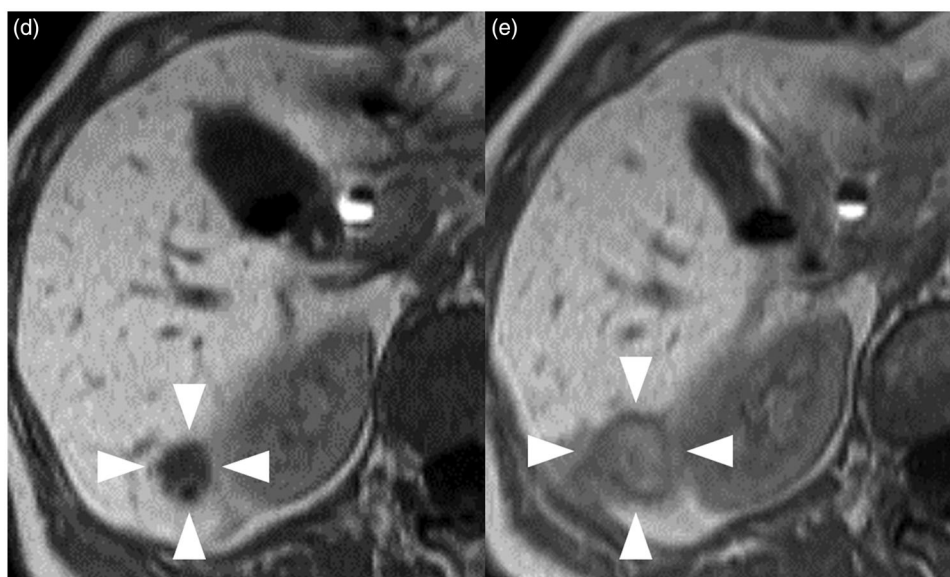


Figure 2. Continued

with a well-defined margin on three-dimensional US images. These marks simultaneously appeared as small green cross marks on both the three-dimensional US and CEUS images, becoming large box marks as the transducer moved. Therefore, while scanning with the GPS marks in place, the lesion could be detected by CEUS at almost the same position as where the GPS marks were observed as green cross marks.

Performing RFA under the guidance of US/US fusion imaging

To use fusion imaging during RFA, the three-dimensional US liver volume data were obtained before RFA under breath-hold (Figure 1(d,e)). The first puncture of the RFA needle was performed under the guidance of real-time conventional US and three-dimensional US fusion imaging using the LOGIQ E9 ultrasound system and a convex probe with a frequency of 1–6 MHz or a micro-convex probe with a frequency of 2–5 MHz (Figure 2(a)). After an RFA procedure, the ablated HCC lesion becomes hyperechoic, which makes it difficult to identify the margin of the target lesion. The second (and third) puncture of the RFA needle was also performed under real-time conventional US and three-dimensional US fusion imaging guidance to ensure accurate puncture of the target lesion. After the initial RFA procedure, as mentioned above, we evaluated the therapeutic efficacy of RFA by CEUS/US fusion imaging because this modality allowed the residual HCC and/or insufficiently ablated areas to be detected. We then performed further ablation if necessary under the guidance of CEUS/US fusion imaging.

One hepatology physician (KN) with more than 10 years of experience in treating HCC by RFA performed all the procedures. RFA was performed under local anesthesia in all cases. The electrode was inserted at different sites, and overlapping ablations were performed until the entire lesion was ablated, as determined by CEUS/US fusion imaging.

Intraprocedural assessment of RFA

Evaluation of therapeutic efficacy using CEUS/US fusion imaging

Immediately (about 5–10 min) after ablation, we confirmed the location of the ablated HCC using CEUS/US fusion imaging with GPS marks, thereby differentiating the ablated HCC from the ablated adjacent liver parenchyma and allowing measurement of the width of the thinnest ablation margin (Figure 2(b,c)). More specifically, we fused the images of the largest cut surface of each lesion obtained by CEUS and the three-dimensional US volume data obtained during a single breath-hold. When the GPS marks were set at the margins of the largest cut surface of the target tumor on the three-dimensional US volume data, the extent of the tumor could be visualized by the locations of the green cross marks on CEUS. When the area of observation moved from the largest cut surface of the tumor to the marginal area or outside of the tumor, the GPS marks changed from green cross marks to box marks. This allowed us to identify the margin of the tumor. Using this procedure, we were able to determine whether the ablation, i.e., the burn, covered the entire tumor area. The CEUS findings were evaluated by two hepatology physicians (KS and KN) to determine the effects of RFA.

The degree of ablation was classified as follows: a 5 mm or larger ablation margin present around the entire tumor (grade A); an ablation margin around the entire tumor but less than 5 mm in diameter in some places (grade B); an incomplete ablation margin around the tumor although no residual tumor apparent (grade C); tumor not completely ablated (grade D) [23]. A grade A evaluation indicated complete ablation whereas grades B–D represented inadequate ablation. However, in the case of HCCs located within 5 mm of relatively large vessels such as the portal vein or of the liver surface, it might not be possible to obtain an ablation margin of ≥ 5 mm diameter; in these cases, grade B was considered to represent adequate ablation.

Table 1. Baseline characteristics of the patients with HCC.^{a,b}

Characteristics	HCC (n = 50)
Number of patients	43
Single lesion/two lesions/three lesions	37/5/1
Age (mean, range; years)	68, 44–88
Sex (male/female)	28/15
Etiology of HCC	
Hepatitis B/hepatitis C/others	11/26/6
Child-Pugh classification	
Class A/B	40/3
Mean diameter of the lesions (range) in mm	15.3 (8–29)
Number of lesions measuring 1–10/11–20/21–30 mm in diameter	9/36/5
Mean follow-up period (range) in months	21.4 (15–27)
Number of lesions locating less than 5mm from vessels/bile duct/liver surface	14/4/5

^aOthers: alcohol, primary biliary cholangitis, idiopathic.

^bVessels: the relatively large vessels such as the portal vein or hepatic vein.

Assessment of technical success and further ablation

If the ablation was evaluated as adequate, we deemed the treatment to be complete. However, if the ablation was evaluated as inadequate, we performed additional ablation under CEUS/US fusion imaging guidance (Figure 2(b)). We considered the treatment as complete if the ablation was evaluated as adequate on CEUS/US fusion imaging (Figure 2(c)); if not, no further ablation was considered possible.

Post-treatment assessment

Evaluation of therapeutic efficacy of RFA by CECT/CEMRI

The final treatment outcome was evaluated by CECT (n = 31) and/or CEMRI (n = 19) performed 1 month after RFA. To determine the effects of RFA, the CECT/CEMRI findings obtained before and after RFA were evaluated by two hepatology physicians (KO and HN), neither of whom was involved in the RFA procedure and both of whom were blinded to all clinical information and radiological findings (Figure 2(d,e)).

Follow-up protocol

All the HCCs that were treated by RFA were followed up by either CECT or CEMRI at 3-monthly intervals. The follow-up period ended in September 2019.

Local tumor progression after RFA

In cases with hypervascular HCC, local recurrence was diagnosed if any enhancement was seen in the margin of the ablated areas in the arterial phase and washout during the subsequent phases on the CECT or CEMRI images. In cases with non-hypervascular HCC, local recurrence was diagnosed when a hypointense lesion was detected adjacent to the ablation zone on images acquired by CEMRI in the hepatobiliary phase. All images were evaluated by two experienced radiologists (HF and MC) working independently and blinded to all clinical information.

Table 2. Mean number of insertions for the initial RFA and additional RFA.

	Initial RFA ^a	Additional RFA ^b	Total
Number of nodules	50	17	50
Mean number of punctures (range) ^c	2.6 (1–6)	1.6 (1–4)	3.2 (1–6)

RFA: radiofrequency ablation.

^aFirst treatment session.

^bAdditional ablation performed immediately after the ablative margin was evaluated as being inadequate by intra-procedural CEUS-US fusion imaging performed at the first treatment session.

^cMean number of insertions of the RFA needle.

Statistical analysis

Using the findings of CECT/CEMRI performed 1 month after RFA as the reference standard, a statistical analysis was performed to calculate the concordance rate for the results of evaluation of the efficacy of RFA between the CECT/CEMRI and CEUS/US fusion imaging. Agreement was graded according to the kappa values (shown within parentheses) as follows: poor (≤ 0.20), fair (0.21–0.40), moderate (0.41–0.60), good (0.61–0.80) or very good (0.81–1.0) [24]. The statistical analyses were performed using statistical software (SPSS version 22; IBM Corp., Armonk, NY).

Results

Patient information

The study included 43 patients (with 50 HCCs). Twenty-seven patients had newly developed recurrent HCC and 16 had newly diagnosed HCC. The characteristics of the patients at baseline are summarized in Table 1.

Evaluation of therapeutic efficacy by CEUS/US fusion imaging immediately after initial RFA

The registration success rate of CEUS/US fusion imaging was 100% (50/50). According to the first evaluation by intraprocedural CEUS/US fusion imaging performed during RFA, 33 HCCs were deemed to have been adequately ablated. The remaining 17 HCCs were evaluated as not having been adequately ablated. The mean number of insertions of the RFA needle for the initial RFA was 2.6 (range 1–6) per tumor (Table 2).

Evaluation of therapeutic efficacy by CEUS/US fusion imaging performed immediately after additional RFA

Seventeen of the 50 HCCs that had been initially evaluated as inadequately ablated underwent further ablation. After additional ablation, 16 of the 17 HCCs were evaluated as adequately ablated by CEUS/US fusion imaging. The remaining HCC (maximum diameter, 27 mm) was evaluated as inadequately ablated at both the initial evaluation and the second evaluation after additional RFA. When this patient was selected as a candidate for RFA, RFA appeared to be the most suitable treatment. However, while waiting for the procedure to be performed, the lesion had grown rapidly and a portion of it came to be located behind the portal vein. This

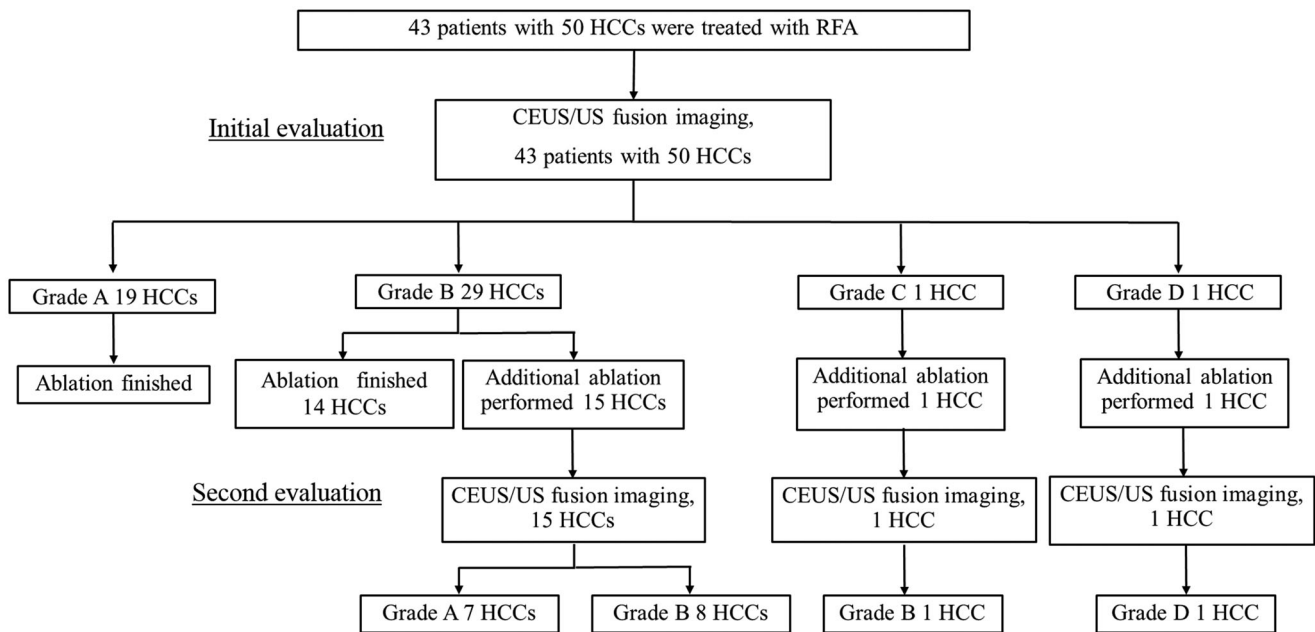


Figure 3. Flow chart of evaluation of therapeutic efficacy of RFA by CEUS/US fusion imaging performed during the RFA procedure.

Table 3. Comparison of evaluation by CEUS-US fusion imaging and CECT/EOB-MRI for assessment of the tumor response after radio-frequency ablation in cases of hepatocellular carcinoma.

US/US fusion	CT/MRI				Tumor (n = 50)
	Grade A ^a	Grade B ^b	Grade C ^c	Grade D ^d	
Grade A	21	3	0	0	24
Grade B	3	22	0	0	25
Grade C	0	0	0	0	0
Grade D	0	0	0	1	1
Total	24	25	0	1	50

^aGrade A (curative): a 5 mm or greater ablative margin around the entire tumor.

^bGrade B (relatively curative): an ablative margin around the tumor, but less than 5 mm in diameter in some places.

^cGrade C (relatively non-curative): only an incomplete ablative margin around the tumor, although no residual tumor was apparent.

^dGrade D (non-curative): the tumor was not completely ablated.

portion could not be ablated adequately. No third ablation was performed because it would have been impossible to maintain an adequate puncture line for RFA. Therefore, this lesion was diagnosed as a residual viable HCC (grade D), and transcatheter arterial chemoembolization was performed 1.5 months after this RFA procedure. The mean number of insertions of the RFA needle for the additional RFA was 1.6 (range 1–4) per tumor (Table 2). All RFA procedures were completed after the initial or second evaluation by CEUS/US fusion imaging (Figure 3).

Complications

All the RFA treatments were performed in a single session without serious adverse events or immediate or late procedure-related complications.

Evaluation of therapeutic efficacy of RFA by intraprocedural CEUS/US fusion imaging performed during RFA compared with that of CECT/CEMRI performed 1 month after RFA

We classified the degree of ablation when the therapeutic efficacy of RFA was evaluated by CEUS/US fusion imaging performed during the RFA procedure and CECT (n = 31) and by CEMRI (n = 19) performed 1 month after RFA (Table 3).

According to the findings on CEUS/US fusion imaging performed during the RFA procedure, the degree of ablation of the HCCs was as follows: grade A, 24 (48%); grade B, 25 (50%); grade C, 0 HCC and grade D, 1 (2%) HCC. Twenty-three of the 25 HCCs that were evaluated as showing grade B ablation were located within 5 mm of relatively large vessels, such as the portal or hepatic vein or from the liver surface, and the remaining two were located behind the puncture line. Therefore, an ablation margin of >5 mm could not be obtained in these lesions.

One case evaluated as showing grade D ablation by CEUS/US fusion imaging was also diagnosed as having residual HCC by CECT/CEMRI performed 1 month after RFA. In contrast, the remaining 49 HCCs were evaluated as showing no residual tumor by CECT/CEMRI performed 1 month after RFA. The concordance rate between the results of evaluation of efficacy of RFA by CECT/CEMRI performed 1 month after RFA was used as the reference standard and CEUS/US fusion imaging performed during the RFA procedure was evaluated. The concordance rate for the HCCs evaluated as showing adequate ablation at the initial evaluation (n = 33) and the HCCs that were adequately ablated only after a second RFA procedure in the same session (n = 17)

was 88% (29/33 in the former category and 15/17 in the latter category; i.e., identical). The overall concordance rate was also 88% (44/50); the kappa value for agreement between the findings of the two imaging modalities was 0.792 (95% confidence interval 0.625–0.960).

Local tumor progression

The mean follow-up period after RFA was 21.4 (range 15–27) months. During this time, the only HCC that was evaluated as showing grade B ablation by both CEUS/US fusion imaging performed during RFA and CEMRI performed 1 month after RFA showed local tumor progression on follow-up CEMRI at 10 months after RFA. This ablated lesion was located adjacent to a large portal vein; therefore, the ablation margin on this side was less than 5 mm. In contrast, the ablation margins on the other sides were more than 5 mm. Local tumor progression in this case arose from areas of the tumor adjacent to the portal vein.

Discussion

In this study, we used CEUS/US fusion imaging (by combining CEUS with Sonazoid and three-dimensional US volume data acquisition by AutoSweep) to evaluate the therapeutic efficacy of RFA. Ninety-eight percent (49/50) of all HCCs were found to have an adequate ablation margin after one or two RFA procedures. Comparison of the results of evaluation of efficacy of RFA between CECT/CEMRI performed 1 month after RFA as the reference standard and CEUS/US fusion imaging performed during the RFA procedure revealed a concordance rate of 88% (44/50). Therefore, CEUS/US fusion imaging during RFA may be a useful method for guiding RFA as well as for evaluating its therapeutic efficacy.

Twenty-three of the 25 HCCs that were evaluated as showing grade B ablation were located within 5 mm of relatively large vessels, such as the portal or hepatic vein or of the liver surface, and a portion of each of the remaining two HCCs was located behind the puncture line. Therefore, an adequate ablation margin of more than 5 mm (grade A) around the entire tumor could not be achieved in 50% (25/50) of the HCCs. However, local recurrence occurred during follow-up (mean 21.4 months; range 15–27 months) in only one of the cases that showed a grade B ablation margin. This lesion was located adjacent to a large portal vein; therefore, the ablation margin on this side was less than 5 mm. The 'cooling effect' of the adjacent large portal vein could have been the reason for local tumor progression in that case. We often encounter cases in which an ablation margin of more than 5 mm around the entire tumor (grade A) cannot be achieved because of the location of the HCC. Therefore, we believe that the findings in this case can be considered clinically representative.

CEUS/US fusion imaging with volume data obtained by AutoSweep three-dimensional US has several advantages. First, the amount of registration error is lower with AutoSweep three-dimensional US than with manual sweep three-dimensional US. When manual sweep

three-dimensional US is used, slight deformation is likely to be seen in about 90-degree rotated plane images from the actual scanned areas. In contrast, no image deformation is seen in AutoSweep three-dimensional US imaging performed to obtain volume data, regardless of the skill of the operator. Consequently, volume data obtained by AutoSweep three-dimensional US are better for guiding RFA and evaluating its therapeutic efficacy. Second, when using this technique, the US volume data as reference are obtained just before the RFA is performed. In contrast, CT or MRI as reference for CEUS/CT or CEUS/MRI fusion imaging is usually performed several days before RFA, when the patient's respiratory status and posture may be slightly different from those during the actual RFA procedure. Moreover, accurate registration between CEUS and CT/MRI is more difficult in patients in whom there has been a rapid increase in ascites and/or rapid growth of the target lesion, deformation of the gallbladder, or disturbance caused by movement of abdominal gas. In contrast, these factors have little impact on CEUS/US fusion imaging. Furthermore, CEUS/US fusion imaging does not involve radiation exposure and can be performed in patients in whom CECT/CEMRI is contraindicated because of contrast allergy or impaired renal function. CEUS/US fusion imaging can also be performed in more patients within a given time period than is possible with CEUS/CECT or CEUS/CEMRI fusion imaging. Third, when the ablation is evaluated as inadequate during the RFA procedure, additional ablation can be undertaken immediately in the same RFA session. These apparent advantages, especially the lack of need for an additional RFA procedure, reduce the physical and mental burden on patients, the length of hospital stay and the treatment-related medical expenses.

In contrast, as with CEUS/CECT or CEMRI fusion imaging, CEUS/US fusion imaging with the volume data obtained by AutoSweep three-dimensional US has some disadvantages. First, breath-hold is necessary for concordance of the images obtained by the two imaging modalities. Registration error occurs, with resulting discordance of the images obtained by the two modalities if the patient cannot hold his/her breath sufficiently. Moreover, registration error is inevitable in any fusion imaging because of the changes in liver morphology caused by respiration and/or slight movements of the patient due to pain during RFA, and adjustments to repair the registration error between the two modalities are needed several times during RFA. In the present study, the discordance rate between CEUS and CECT/CEMRI was found to be 12% (6/50), which may have been due to registration errors caused by the various factors mentioned above. For patients who cannot hold their breath sufficiently, it would be useful if a motion tracking system could be developed in the near future to compensate for the movements of the tumor with respiration so as to maintain concordance between CEUS and other US images [25]. Second, for US technicians who are not familiar with fusion imaging, it takes some time (2–3 min) to achieve adequate registration between these modalities. Auto-registration between the two modalities would be useful to resolve this problem [26].

The present study also has several limitations. First, the volume data were obtained by AutoSweep three-dimensional US. A three-dimensional US probe is slightly thick so is not suitable for guiding accurate puncture, for which a two-dimensional convex probe was used in this study. When a probe of a different shape is placed on the patient's skin, the scanning probe angle becomes slightly different, which could induce registration error between probes of different shapes. In the future, this problem may be resolved if it becomes possible to use phased array transducers that provide three-dimensional information automatically by electronic scanning [27]. Second, while the registration success rate was 100% in this study, because the inclusion criterion for the target HCCs was a well-defined margin on conventional US (78.5% [73/93]), it was still impossible to evaluate the efficacy of RFA in cases where the HCC was deep-seated in relation to the skin surface [9.7% (9/93)] because of US attenuation and disruption caused by the tumor being located near bowel gas. Third, HCCs showing an unclear margin on conventional US [21.5% (20/93)] were excluded. However, if an unclear lesion appeared as a defective area in the post-vascular phase of CEUS imaging, this image is obtained as volume data and used as a reference image, intraprocedural CEUS/CEUS fusion imaging during RFA is possible for RFA guidance and evaluation of the therapeutic efficacy of RFA. Fourth, the patient sample size was relatively small. Further studies are needed to assess whether this novel evaluation modality, which can be applied immediately after RFA, can eliminate the need for evaluation by CECT or CEMRI 1 month after RFA.

Conclusion

Use of fusion imaging that combines CEUS and AutoSweep three-dimensional US to obtain volume data appears to be a useful method for RFA guidance and evaluation of the therapeutic efficacy of RFA for HCCs with a well-defined margin on conventional US.

Acknowledgements

The authors thank all the participating clinicians for their support.

Declaration statement

No potential conflict of interest was reported by the author(s).

References

- [1] Kim SK, Lim HK, Kim YH, et al. Hepatocellular carcinoma treated with radio-frequency ablation: spectrum of imaging findings. *Radiographics*. 2003;23(1):107–121.
- [2] Lim HK, Choi D, Lee WJ, et al. Hepatocellular carcinoma treated with percutaneous radio-frequency ablation: evaluation with follow-up multiphase helical CT. *Radiology*. 2001;221(2):447–454.
- [3] Passera K, Selvaggi S, Scaramuzza D, et al. Radiofrequency ablation of liver tumors: quantitative assessment of tumor coverage through CT image processing. *BMC Med Imaging*. 2013;13(1):3.
- [4] Sakakibara M, Ohkawa K, Katayama K, et al. Three-dimensional registration of images obtained before and after radiofrequency ablation of hepatocellular carcinoma to assess treatment adequacy. *AJR Am J Roentgenol*. 2014;202(5):487–495.
- [5] Claudon M, Dietrich CF, Choi BI, et al. Guidelines and good clinical practice recommendations for contrast enhanced ultrasound (CEUS) in the liver-update 2012: a WFUMB-EFSUMB initiative in cooperation with representatives of AFSUMB, AIUM, ASUM, FLAUS and ICUS. *Ultrasound Med Biol*. 2013;39(2):187–210.
- [6] Westwood M, Joore M, Grutters J, et al. Contrast enhanced ultrasound using SonoVue® (sulphur hexafluoride microbubbles) compared with contrast-enhanced computed tomography and contrast-enhanced magnetic resonance imaging for the characterisation of focal liver lesions and detection of liver metastases: a systematic review and cost-effectiveness analysis. *Health Technol Assess*. 2013;17(16):1–243.
- [7] Wiesinger I, Wiggermann P, Zausig N, et al. Percutaneous treatment of malignant liver lesions: evaluation of success using contrast-enhanced ultrasound (CEUS) and perfusion software. *Ultraschall Med*. 2018;39(4):440–447.
- [8] Wen YL, Kudo M, Zheng RQ, et al. Radiofrequency ablation of hepatocellular carcinoma: therapeutic response using contrast-enhanced coded phase-inversion harmonic sonography. *AJR Am J Roentgenol*. 2003; 181(1):57–63.
- [9] Kisaka Y, Hirooka M, Kumagi T, et al. Usefulness of contrast-enhanced ultrasonography with abdominal virtual ultrasonography in assessing therapeutic response in hepatocellular carcinoma treated with radiofrequency ablation. *Liver Int*. 2006;26(10):1241–1247.
- [10] Numata K, Fukuda H, Morimoto M, et al. Use of fusion imaging combining contrast-enhanced ultrasonography with a perflubutane-based contrast agent and contrast-enhanced computed tomography for the evaluation of percutaneous radiofrequency ablation of hypervascular hepatocellular carcinoma. *Eur J Radiol*. 2012;81(10):2746–2753.
- [11] Hao Y, Numata K, Ishii T, et al. Rate of local tumor progression following radiofrequency ablation of pathologically early hepatocellular carcinoma. *World J Gastroenterol*. 2017;23(17):3111–3121.
- [12] Nishigori S, Numata K, Irie K, et al. Fusion imaging with contrast-enhanced ultrasonography for evaluating the early therapeutic efficacy of radiofrequency ablation for small hypervascular hepatocellular carcinomas with iso-echoic or unclear margins on conventional ultrasonography. *J Med Ultrasonics*. 2018;45(3):405–415.
- [13] Makino Y, Imai Y, Igura T, et al. Feasibility of extracted-overlay fusion imaging for intraoperative treatment evaluation of radiofrequency ablation for hepatocellular carcinoma. *Liver Cancer*. 2016;5(4):269–279.
- [14] Ma QP, Xu EJ, Zeng QJ, et al. Intraprocedural computed tomography/magnetic resonance-contrast-enhanced ultrasound fusion imaging improved thermal ablation effect of hepatocellular carcinoma: comparison with conventional ultrasound. *Hepatol Res*. 2019;49(7):799–809.
- [15] Xu EJ, Lv SM, Li K, et al. Immediate evaluation and guidance of liver cancer thermal ablation by three-dimensional ultrasound/contrast-enhanced ultrasound fusion imaging. *Int J Hyperthermia*. 2018;34(6):870–876.
- [16] Kudo M, Matsui O, Izumi N, et al. JSH consensus-based clinical practice guidelines for the management of hepatocellular carcinoma: 2014 update by the liver cancer study group of Japan. *Liver Cancer*. 2014;3(3–4):458–468.
- [17] Sugimori K, Numata K, Okada M, et al. Central vascular structures as a characteristic finding of regenerative nodules using hepatobiliary phase gadolinium ethoxybenzyl diethylenetriaminepenta-acetic acid-enhanced MRI and arterial dominant phase contrast-enhanced US. *J Med Ultrasonics*. 2017;44(1):89–100.
- [18] Numata K. Advances in ultrasound systems for hepatic lesions in Japan. *J Med Ultrasonics*. 2015;42(3):297–301.
- [19] Numata K, Fukuda H, Miwa H, et al. Contrast-enhanced ultrasonography findings using a perflubutane-based contrast agent in patients with early hepatocellular carcinoma. *Eur J Radiol*. 2014; 83(1):95–102.
- [20] Numata K, Fukuda H, Nihonmatsu H, et al. Use of vessel patterns on contrast-enhanced ultrasonography using a

- perflubutane-based contrast agent for the differential diagnosis of regenerative nodules from early hepatocellular carcinoma or high-grade dysplastic nodules in patients with chronic liver disease. *Abdom Imaging*. 2015;40(7):2372–2383.
- [21] Ishii T, Numata K, Hao Y, et al. Evaluation of hepatocellular carcinoma tumor vascularity using contrast-enhanced ultrasonography as a predictor for local recurrence following radiofrequency ablation. *Eur J Radiol*. 2017;89:234–241.
- [22] Kunishi Y, Numata K, Morimoto M, et al. Efficacy of fusion imaging combining sonography and hepatobiliary phase MRI with Gd-EOB-DTPA to detect small hepatocellular carcinoma. *AJR Am J Roentgenol*. 2012;198(1):106–114.
- [23] Nishikawa H, Osaki Y, Iguchi E, et al. Radiofrequency ablation for hepatocellular carcinoma: the relationship between a new grading system for the ablative margin and clinical outcomes. *J Gastroenterol*. 2013;48(8):951–965.
- [24] Altman DG. *Practical statistics for medical research*. London: Chapman & Hall; 1991. p. 1–611.
- [25] Seo J, Koizumi N, Funamoto T, et al. Visual serving for a US-guided therapeutic HIFU system by coagulated lesion tracking: a phantom study. *Int J Med Robotics Comput Assist Surg*. 2011; 7(2):237–247.
- [26] Cha DI, Lee MW, Song KD, et al. A prospective comparison between auto-registration and manual registration of real-time ultrasound with MR images for percutaneous ablation or biopsy of hepatic lesions. *Abdom Radiol*. 2017;42(6):1799–1808.
- [27] Huang Q, Zeng Z. A review on real-time 3d ultrasound imaging technology. *Biomed Res Int*. 2017;2017:1–20.

論文目録

I 主論文

Use of intra-procedural fusion imaging combining contrast-enhanced ultrasound using a perflubutane-based contrast agent and auto sweep three-dimensional ultrasound for guiding radiofrequency ablation and evaluating its efficacy in patients with hepatocellular carcinoma

Sanga, K., Numata K., Nihonmatsu, H., Ogushi, K., Fukuda, H., Chuma, M., Hashimoto, H, Koizumi, N., Maeda, S

International Journal of Hyperthermia vol.37, (1), 202-211, 2020

II 副論文

なし

III 参考論文

なし